

# Barrier-Controlled Non-Equilibrium Criticality in Reactive Particle Systems

Qun-Li Lei,<sup>1</sup> Hao Hu,<sup>2</sup> and Ran Ni<sup>1,\*</sup>

<sup>1</sup>*School of Chemical and Biomedical Engineering,*

*Nanyang Technological University, 62 Nanyang Drive, 637459, Singapore*

<sup>2</sup>*School of Physics and Materials Science, Anhui University, Hefei 230601, China*

Non-equilibrium critical phenomena generally exist in many dynamic systems, like chemical reactions and some driven-dissipative reactive particle systems. Here, by using computer simulation and theoretical analysis, we demonstrate the crucial role of the activation barrier on the criticality of dynamic phase transitions in a minimal reactive hard-sphere model. We find that at zero thermal noise, with increasing the activation barrier, the type of transition changes from a continuous conserved directed percolation into a discontinuous dynamic transition by crossing a *tricritical* point. A mean-field theory combined with field-simulation is proposed to explain this phenomenon. The possibility of Ising-type criticality in the non-equilibrium system at finite thermal noise is also discussed.

## INTRODUCTION

Non-equilibrium critical phenomena [1, 2] generically exist in various systems, e.g., chemical reactions [3, 4], epidemic spreads [5], brain activities [6], colloidal and granular systems [7–10], turbulence and active fluids [11–16] etc. At the critical point, these systems exhibit scaling-invariance accompanied by diverging correlation lengths and time scales, which can be characterized by some generic critical exponents [2]. The directed percolation (DP) exemplified by the lattice contact model [17] is among the best-known universality classes of non-equilibrium phase transitions, yet deviations from the DP universality are also found in many dynamic systems [2]. For examples, by introducing particle number conservation, a new universality of conserved direction percolation (C-DP) was found in the Manna model [18] and conserved lattice gas model [19], while in the Schlogl’s second model aiming to model the cooperative surface catalytic reaction, the dynamic transition becomes first-order [3]. Nevertheless, lattice models are usually over-simplified and may neglect some key mechanisms in real dynamic critical systems, e.g., chemical reactions, in which the kinetic energy, particle inertia, momentum conservation and some barrier-crossing processes play important roles. Thus, it remains unclear whether there is any overlooked but fundamental mechanism controlling the non-equilibrium criticality in those real dynamic systems.

To this end, here we investigate a minimal reactive hard sphere model with an activation barrier, which captures the essential physics of many non-equilibrium particle systems. For examples, this model can be regarded as a simplified version of the Semenov hard sphere model for exothermic chemical reactions [20–23]. The Semenov model, which assumes a uniform temperature distribution and neglects the reactant consumption at ignition, is a classical theory of thermal explosion [24, 25]. Our model can also be viewed as a modification of random-organization hard sphere model with the addition of an activation barrier. The random-organization was origi-

nally proposed to model colloidal particle system under oscillatory shearing [7, 8, 26–28], while it exhibits generic non-equilibrium critical behavior, which has connections with the yielding of amorphous solids [9, 29], the jamming transition [30–34], depinning transition [35–37] and dynamic hyperuniform states [38–43] etc. By using simulation and theory, we prove that the activation barrier controls the criticality or “sharpness” of the no-equilibrium phase transition in the system: at zero thermal noise, increasing the activation barrier changes the type of absorbing transition from a continuous C-DP to a discontinuous dynamic transition by crossing a *tricritical* point. We propose a mean-field theory combined with field-simulation to explain this phenomenon. The mean-field analysis also indicates that the non-equilibrium transition at finite thermal could be Ising-type.

## RESULTS

### Model and Simulation

The model we consider consists of  $N$  hard spheres with the same mass  $m$  and diameter  $\sigma$ . Activations occur in pairwise collisions between two particles  $i, j$ , if their relative distance approaches  $\sigma$  and relative kinetic energy along the center-to-center direction surpasses the activation barrier  $E_b$ , i.e.,

$$|\Delta \mathbf{r}_{i,j}| = \sigma \quad (1)$$

$$\frac{1}{2}m(\Delta v_{i,j}^\perp)^2 > E_b \quad (2)$$

where  $\Delta \mathbf{r}_{i,j} = \mathbf{r}_j - \mathbf{r}_i$  is the relative distance between two particles and

$$\Delta v_{i,j}^\perp = \Delta \mathbf{v}_{i,j} \cdot \frac{\Delta \mathbf{r}_{i,j}}{\sigma} \quad (3)$$

is the relative velocity along the center-to-center direction with  $\Delta \mathbf{v}_{i,j} = \mathbf{v}_j - \mathbf{v}_i$  the relative velocity. During each activation, additional kinetic energy  $\epsilon$  is released,

with the momentum of the two particles conserved. We assume a frictionless collision, thus the velocity change for particle  $i, j$  during the collision is

$$\mathbf{u}_i = -\mathbf{u}_j = \frac{\Delta v_{i,j}^\perp - \sqrt{(\Delta v_{i,j}^\perp)^2 + 4\epsilon/m} \frac{\Delta \mathbf{r}_{i,j}}{\sigma}}{2}. \quad (4)$$

Between two consecutive collisions, the motion of particles obeys the Langevin dynamics. For particle  $i$ , the equation of motion can be written as

$$m \frac{d\mathbf{v}_i(t)}{dt} = -\gamma \mathbf{v}_i(t) + \sqrt{2\gamma k_B T} \eta(t), \quad (5)$$

where  $\gamma$  is the damping coefficient. The second noise term is based on the fluctuation-dissipation theorem with  $T$  the thermal temperature and  $\eta(t)$  the Gaussian white noise. This model is a direct generalization of the random-organizing hard-sphere model with the addition of an activation barrier and thermal noise, which can be realized by using active spinners with short-range repulsion [42]. It can also be seen as a simplified version of the Semenov reactive hard-sphere model for exothermic chemical reactions, in which non-consumable reactants are confined by two parallel walls connected with thermal reservoir at a fixed temperature [20–23], whereas the boundary thermalization is treated implicitly through a Langevin thermostat in our model.

We adopt the Langevin dynamic event-driven simulation to simulate this system. The evolution of the velocities and positions of particles, as well as the collisions between particles, are all deterministic in the absence of thermal noise. The prediction of collisions and event-management are well documented in Ref. [42, 44]. In the presence of the thermal noise, thermalization events are added to the event calendar after every time step  $\Delta t = \tau_d/10$ , where  $\tau_d = m/\gamma$  is the typical dissipation time. The velocity of particle  $i$  in the case of no collision is updated according to [45]

$$v_{i,\alpha}(t + \Delta t) = e^{-\frac{\gamma}{m}\Delta t} v_{i,\alpha}(t) + \sqrt{v_{th}^2 (1 - e^{-2\frac{\gamma}{m}\Delta t})} \eta(\mathbf{r}, t) \quad (6)$$

where  $\alpha = x, y, z$  and  $v_{th}^2 = dk_B T/m$ . The dimensionality of the system we study is  $d=2, 3$  with periodic boundary conditions in all directions. The reduced particle density of the system is defined as  $\tilde{\rho} = N\sigma^d/V$  with  $V = L^d$  the volume of the system and  $L$  the box length. The typical excitation speed is defined as  $v_0 = \sqrt{\epsilon/m}$ , and the time unit of the system is set as  $\tau_0 = \sigma/v_0$ .

### Critical phenomena

We first study the 2D system at zero thermal noise  $T=0$ . In this case, as shown in Ref [42], there are two important characteristic lengths in the system, i.e., the

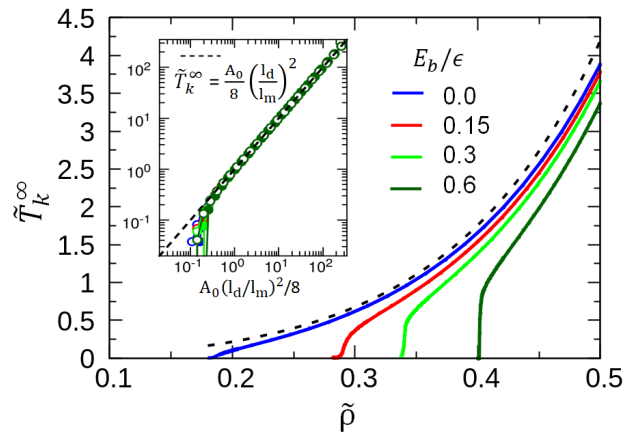


FIG. 1: steady-state kinetic temperature  $\tilde{T}_k^\infty$  as a function of density for 2D system with different  $E_b$ . Inset:  $\tilde{T}_k^\infty$  as a function of  $l_d$  ( $\tilde{\rho}=0.1$ , solid symbols) and  $l_m$  ( $l_d=160\sigma$ , open symbols). The dashed lines are the theoretical predictions with  $A_0=1.56$ .

mean free path  $l_m$  and the dissipation length  $l_d = \sqrt{m\epsilon}/\gamma$ . The latter is the typical distance that an isolated particle can travel after being activated by collision. The system undergoes a dynamic absorbing-active phase transition at  $l_d \simeq l_m$  [42]. Here, the absorbing state corresponds to the zero kinetic energy state or zero kinetic temperature  $T_k=0$ , while the active state has a finite kinetic energy ( $T_k > 0$ ). The kinetic temperature of the system  $T_k$  is different from  $T$ , which reflects the strength of thermal noise. Thus, the reduced kinetic temperature of the system can be chosen as the order parameter of the system, i.e.,

$$\tilde{T}_k(t) = \frac{dk_B T_k(t)}{\epsilon} \quad \text{and} \quad k_B T_k(t) = \frac{m \langle v^2(t) \rangle}{d}. \quad (7)$$

Here,  $\overline{v^2}$  is the average square of speed of all particles and  $\langle \cdot \rangle$  calculates the ensemble average of active (surviving) trials [19]. In Fig. 1, we plot the steady-state kinetic temperature  $\tilde{T}_k^\infty \equiv \tilde{T}_k(t \rightarrow \infty)$  as a function of density for systems with different activation barriers. With increasing  $E_b$ , the transition shifts to the higher density regime and becomes sharper, similar to the explosive percolation [46]. Same phenomenon is also found in 3D systems as shown Fig. S1 in Ref. [47].

To determine the type of the transitions, we assume there is a scaling-invariant critical point  $\tilde{\rho}_c$  in the system and perform finite-size analysis to determine  $\tilde{\rho}_c$  and the corresponding critical exponents. For systems near the critical point,  $\tilde{T}_k^\infty(\Delta\tilde{\rho}, L)$  satisfies the scaling relationship [2, 19],

$$\tilde{T}_k^\infty(\Delta\tilde{\rho}, L) = L^{-\beta/\nu_\perp^*} \mathcal{G}\left(L^{1/\nu_\perp^*} \Delta\tilde{\rho}\right), \quad (8)$$

where  $\Delta\tilde{\rho} = \tilde{\rho} - \tilde{\rho}_c$  and  $\mathcal{G}(\cdot)$  is the scaling function.  $\nu_\perp^*$  normally equals  $\nu_\perp$  in the scaling relationship of spatial correlation length  $\xi_\perp \sim |\Delta\tilde{\rho}|^{-\nu_\perp}$  [42]. For systems at the

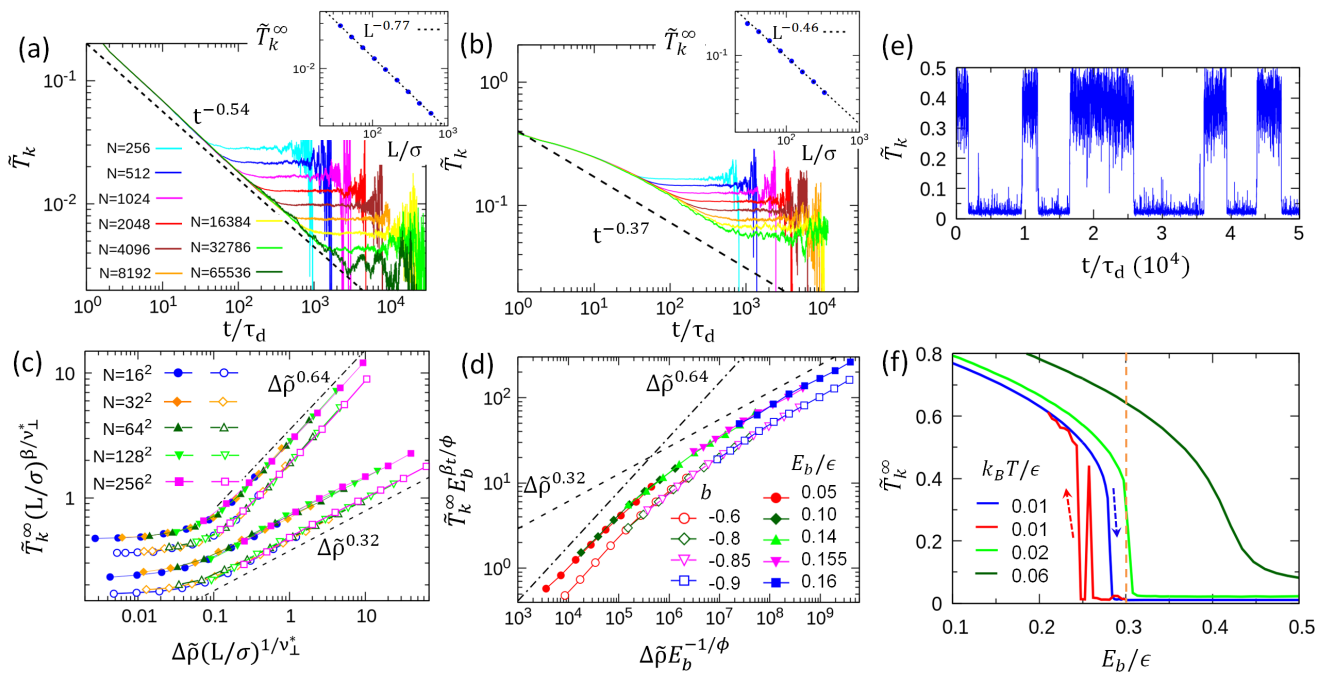


FIG. 2: Barrier-controlled critical behaviors in 2D systems. (a, b)  $\tilde{T}_k$  as a function of time for different system sizes with inset showing saturated value as a function of system size at zero thermal noise. (a)  $E_b=0$ ,  $\bar{\rho}=0.18471$ ; (b)  $E_b=0.165\epsilon$ ,  $\bar{\rho}=0.29615$ . (c) Collapse of  $\tilde{T}_k(\Delta\bar{\rho})$  according to Eq. (8) for different system sizes at zero thermal noise. Solid symbols are for reactive hard-sphere systems with  $E_b=0.0$  (upper),  $0.165\epsilon$  (lower), respectively. The open symbols are obtained in field simulations of Eq. (26-27) with  $b=1$  (upper),  $-0.92$  (lower), respectively. (d) Crossover scaling analysis of the tricritical point based on Eq (10) at zero thermal noise. (e) Demonstration of bistability at  $E_b=0.3\epsilon$ ,  $\bar{\rho}=0.3290$  with thermal noise  $k_B T=0.02\epsilon$  for a system with  $N=1024$ . (f)  $\tilde{T}_k$  as a function of reaction barrier  $E_b$  at different thermal temperature  $T$  for 2D hard sphere systems at density  $\bar{\rho}=0.3290$  and  $N=1024$ . Hysteresis loop is found in system at  $k_B T=0.01\epsilon$  starting from different initial states as indicated by the dashed arrows. The yellow line indicates the density point at which the system exhibits clear bistability in (e).

critical point ( $\Delta\bar{\rho}=0$ ), starting from random initial configurations,  $\tilde{T}_k(t)$  follows a power-law decay  $t^{-\alpha}$  before reaching the saturated value satisfying  $\tilde{T}_k^\infty \sim L^{-\beta/\nu_\perp^*}$ . In all our simulations, we use natural homogeneous initial configurations [48], which have been shown able to avoid the anomalous undershooting and lead to a more self-consistent  $\alpha$  exponent compared with complete random initial configurations [48, 49]. In Fig. 2a, we show the decay of  $\tilde{T}_k(t)$  for a 2D system of different size  $L \propto N^{1/d}$  for  $E_b=0$  and  $l_d=2\sigma$ . The inset plots  $\tilde{T}_k^\infty$  as a function of  $L$ . Both figures indicate the scaling-invariance and we obtain the corresponding critical exponents  $\alpha=0.54$  and  $\beta/\nu_\perp^*=-0.77$ . In Fig. 2c, we plot the collapse of  $\tilde{T}_k^\infty(\Delta\bar{\rho}, L)$  for different  $L$  (solid symbols) based on Eq. (8) with  $\beta=0.64$  and  $\nu_\perp^*=0.84$ , which is consistent with the obtained  $\beta/\nu_\perp^*$ .

At the critical state, one can also define the overall activity  $\psi_a$ , which has the same definition as  $\tilde{T}_k$  except that the data are averaged over both surviving and non-surviving trials [19].  $\psi_a$  obeys another finite-size scaling

$$\psi_a(t, L) = t^{-\alpha} \mathcal{F}(tL^{-z^*}) \quad (9)$$

with  $\mathcal{F}(\cdot)$  the scaling function. Here  $z^* = \nu_\parallel/\nu_\perp^*$  is the dynamic exponent with  $\nu_\parallel$  originating from the scaling

relationship of temporal correlation length,  $\xi_\parallel \sim |\Delta\bar{\rho}|^{-\nu_\parallel}$ . In Fig. 3a,b, by using this finite-size scaling method, we obtain  $z=1.50$ .

All the critical exponents we obtain at  $E_b=0$  and zero thermal noise for both 2D and 3D systems are summarized in Table I, which indicates that the criticality of this phase transition belongs to C-DP or Manna class [18, 42]. Nevertheless, with a similar analysis for 2D systems of  $E_b=0.165\epsilon$  in Fig. 2b,d and Fig. 3c,d, we obtain critical exponents distinct from C-DP (Table I). Same finding applies to 3D systems as shown in Fig. S2-S3 in Ref. [47]. As shown later, these unreported exponents appear because the system is at a *tricritical* point, which separates the continuous and discontinuous transitions. Indeed, by further increasing  $E_b$  to  $0.3\epsilon$ , we find the finite-size scaling breaks down and the 2D system exhibits the bistability if turning on the thermal noise to  $k_B T=0.02\epsilon$  (Fig. 2e). In Fig. 2f, we further show the appearance of cusp bifurcation and hysteresis loop with increasing the activation barrier at finite thermal noise. Therefore, the system undergoes a discontinuous transition at large activation barrier even with a finite thermal noise.

To determine the tricritical point at the zero thermal noise, we employ a crossover scaling analysis [50–52]. Supposing  $E_{b,c}$  is the tricritical energy barrier and letting

$\Delta E_b = E_b - E_{b,c}$ , the crossover scaling can be written as

$$\tilde{T}_k(\Delta\tilde{\rho}, \Delta E_b) = \Delta E_b^{-\beta_t/\phi} \mathcal{G}_t(\Delta\tilde{\rho}\Delta E_b^{-1/\phi}), \quad (10)$$

given  $\Delta\tilde{\rho} \ll \Delta E_b/\epsilon$  [50]. Here, the scaling function  $\mathcal{G}_t(x) \sim x^\beta$  when  $x \ll 1$  and  $\mathcal{G}_t(x) \sim x^{\beta_t}$  when  $x \gg 1$  with  $\beta_t$  the tricritical exponent. In Fig. 2d, we show the collapse of  $\tilde{T}_k(\Delta\tilde{\rho})$  for 2D systems with different  $E_b$  (solid symbols), which leads to  $E_{b,c} = 0.165\epsilon$  and  $\phi = 0.32$ . Similar collapsing can be made to determine the tricritical point in 3D systems as shown in Fig S2 in Ref. [47].

2D					
	$\beta_{(t)}$	$\alpha$	$\nu_\perp^*$	$z^*$	$\phi$
C-DP	0.64(1)	0.52(1)	0.80(2)	1.53(2)	
$E_b = 0$	0.64(2)	0.54(2)	0.84(3)	1.50(3)	
$b = 1$	0.65(2)	0.53(2)	0.84(3)	1.51(2)	
$E_b = E_{b,c}$	0.32(4)	0.37(5)	0.68(4)	1.68(5)	0.32(5)
$b = b_c$	0.33(3)	0.36(4)	0.70(3)	1.65(5)	0.34(4)
3D					
	$\beta_{(t)}$	$\alpha$	$\nu_\perp^*$	$z^*$	$\phi$
C-DP	0.84(1)	0.75(2)	0.59(1)	1.82(2)	
$E_b = 0$	0.85(3)	0.86(2)	0.60(2)	1.79(4)	
$b = 1$	0.86(3)	0.86(2)	0.59(3)	1.78(3)	
$E_b = E_{b,c}$	0.48(3)	0.52(4)	1.0(4)	1.95(6)	0.50(5)
$b = b_c$	0.50(2)	0.51(3)	0.95(5)	2.0(4)	0.50(4)
Mean field	1/2	1/2	1	2	1/2

TABLE I: Critical exponents in 2D and 3D systems. Data for C-DP is from [2, 49]. Different values of  $E_b$  and  $b$  are for reactive hard-sphere model and field simulations of Eq. (26-27), respectively. Tricritical points for 2D system are at  $E_{b,c} = 0.165(5)\epsilon$  and  $b_c = -0.92(3)$ . Tricritical points for 3D system at  $E_{b,c} = 0.070(3)\epsilon$  and  $b_c = -0.35(2)$ . Note that in 3D case, the  $\alpha$  is larger than the reference value because we use natural homogeneous initial configurations in our simulations [48, 49].

### General theoretical analysis

To understand the complex phase behaviour above, we first analyse the variables, intrinsic symmetries, conservation laws, and forms of fluctuations in the system: i) generally, the system is described by three hydrodynamic variables, i.e., the density field, the velocity field and the energy field. However, since the velocity field is damped, it is no longer an independent variable in the hydrodynamic limit; ii) the system is spatially isotropic, so the gradient terms in the dynamic equation must be even; iii) the system conserves the particle number, but does not conserve the momentum and energy; iv) the fluctuations come from two parts: one is from the thermal excitation whose variance is proportional to the thermal temperature  $T$ , the other is from collision activations with

the variance proportional to the kinetic temperature  $T_k$ . As a result, the dynamic equations for the left two independent variables, local energy (kinetic temperature) field  $\tilde{T}_k^l(\mathbf{r}, t)$  and local density field  $\tilde{\rho}_l(\mathbf{r}, t)$  of the system should have the form

$$\frac{\partial \tilde{T}_k^l}{\partial t} = \mu \nabla^2 \tilde{T}_k^l + F(\tilde{T}_k^l, \tilde{\rho}_l, T) + \Lambda \sqrt{\tilde{T}_k^l} \eta(\mathbf{r}, t) \quad (11)$$

$$\frac{\partial}{\partial t} \tilde{\rho}_l = \nabla \cdot \mathbf{J}(\tilde{T}_k^l, \tilde{\rho}_l) + \nabla \cdot \boldsymbol{\xi}(\mathbf{r}, t). \quad (12)$$

Here, the second equation is a result of particle number conservation. Function  $F$  and current  $\mathbf{J}$  can be arbitrary functions of  $\tilde{\rho}$ ,  $\tilde{T}_k$ ,  $T$  and their spatial derivatives.  $\Lambda$  is the strength of Gaussian white noise  $\eta(\mathbf{r}, t)$ . Noise  $\boldsymbol{\xi}(\mathbf{r}, t)$  satisfying  $\langle \xi_i(\mathbf{r}, t) \xi_j(\mathbf{r}', t') \rangle = 2\Gamma \tilde{\rho} k_B T \delta_{ij} \delta(\mathbf{r} - \mathbf{r}') \delta(t - t')$ . Near the critical point, only the leading terms in  $F$  and current  $\mathbf{J}$  are important. Without thermal excitation  $\boldsymbol{\xi}(\mathbf{r}, t) = 0$ , the mass transport can only happen when both  $\tilde{T}_k$  and  $\tilde{\rho}$  are non-zero, thus the leading terms in  $\mathbf{J}$  would be proportional to  $\tilde{T}_k \nabla \tilde{\rho}$  and  $\tilde{\rho} \nabla \tilde{T}_k$ .

### Mean-field theory

Now we obtain the expression for  $F(\tilde{T}_k, \tilde{\rho}, T)$  from the kinetic point of view. At the mean-field level, the activation driving power  $W_{driv}$  and the dissipation power  $W_{disp}$  per particle are [42]

$$W_{driv} = f_a \epsilon, \quad W_{disp} = \bar{v}^2 \gamma \quad (13)$$

respectively. Here,  $f_a$  is the average activating collision frequency per particle which can be written as

$$f_a = x_a \bar{v}_a / (2l_r), \quad (14)$$

with  $x_a$  the fraction of activated particles and  $\bar{v}_a$  is the average speed of activated particles.  $l_r$  is the mean free path of activating collisions. At  $E_b = 0$ ,  $l_r$  equals the mean free path of the system  $l_m$  since every collision induces an activation, while for  $E_b > 0$ , one can expect  $l_r > l_m$  as discussed latter. Moreover, the driving power of thermal noise per particle  $W_{driv}^{therm}$  can be approximated by the equilibrium dissipation power  $W_{disp}^{therm} = \gamma dk_B T / m$ . Thus, by neglecting the fluctuation, the mean-field dynamic equation for  $\tilde{T}_k$  can be written as

$$\begin{aligned} \epsilon \frac{\partial \tilde{T}_k}{\partial t} &= W_{driv} - W_{disp} + W_{driv}^{therm} \\ &= \frac{x_a \tilde{\rho}_r \bar{v}_a \epsilon}{2\sigma} - \gamma \bar{v}^2 + \frac{\gamma dk_B T}{m}. \end{aligned} \quad (15)$$

Here we use the low density approximation for the mean free path of activating collision  $l_r \simeq \sigma / \tilde{\rho}_r$  with  $\tilde{\rho}_r$  the density of effective reactant, i.e., the average density of particle that can be activated under  $\tilde{T}_k$ . For systems far

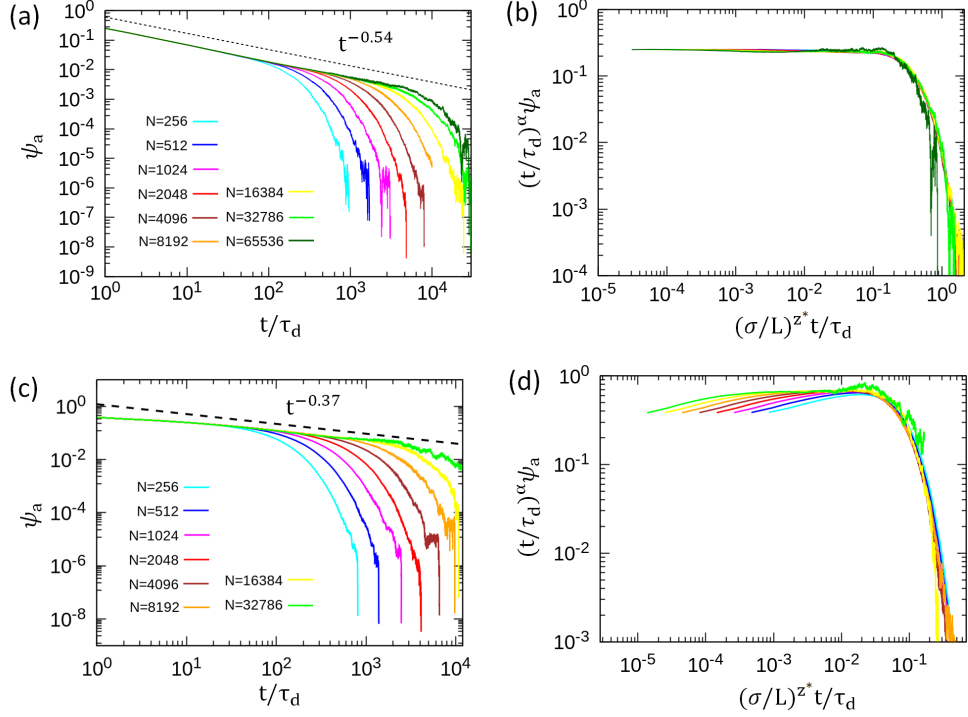


FIG. 3: Overall activity  $\psi_a(t)$  for different system sizes in 2D hard sphere systems at  $E_b=0$ ,  $\tilde{\rho}=0.18471$ . (b) Collapse of activity  $\psi_a(t)$  based on Eq.(9) with  $\alpha=0.54$ ,  $z^*=1.50$ . (c) Overall activity  $\psi_a(t)$  for different system sizes in 2D at tricritical point  $E_b=0.165\epsilon$ ,  $\tilde{\rho}=0.29615$ . (d) Collapse of activity  $\psi_a(t)$  with  $\alpha=0.37$ ,  $z^*=1.68$ .

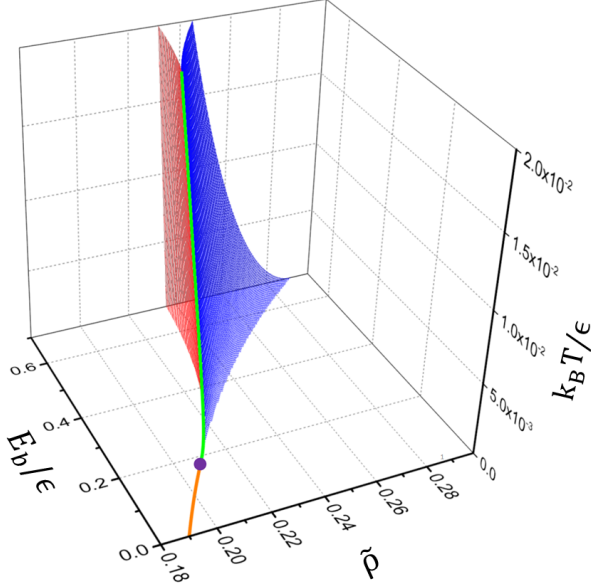


FIG. 4: Mean-field phase diagram. The orange line and green line represent of the C-DP and Ising-type critical points of the system, respectively. The purple point is the tricritical point. The bistability region is enclosed by the blue and red surfaces. The parameters used is  $A=0.095$ ,  $B=1/2$  and  $\tau_d/\tau_0=10$ .

from the critical point ( $l_d \gg l_m$ ) the average kinetic en-

ergy would be much larger than the activation barrier ( $\tilde{T}_k \gg E_b/\epsilon$ ), thus we have  $\tilde{\rho}_r \simeq \tilde{\rho}$ ,  $x_a \simeq 1$  and  $\bar{v}_a \simeq \bar{v}$  with  $\bar{v}$  the average speed of all particles. Based on the approximation  $\bar{v}^2 \simeq \bar{v}^2 = dk_B T_k/m$ , at zero thermal noise  $T=0$ , the steady-state kinetic temperature  $\tilde{T}_k^\infty$  satisfying  $\frac{\partial \tilde{T}_k}{\partial t} = 0$  can be obtained as [42]

$$\tilde{T}_k^\infty \simeq \frac{1}{4d} \left( \frac{l_d}{l_m} \right)^2, \quad (16)$$

which does not depend on  $E_b$ . This is verified in simulations as shown in the inset of Fig. 1. Nevertheless, for systems close to the critical point, there is strong dynamic heterogeneity, i.e., most particles are immobile and only a small fraction of particles are activated with typical excitation speed  $\bar{v}_a \simeq v_0$ . Apparently,  $\bar{v}_a$  is a convex instead of concave function of  $x_a$ , since increasing  $x_a$  also increases the collision between activated particles, further raising  $\bar{v}_a$ . Thus, as a first-order approximation, we have

$$\bar{v}_a \simeq (1 + Ax_a)v_0 \quad (17)$$

$$\tilde{T}_k \simeq x_a m \bar{v}_a^2 / \epsilon \simeq x_a + 2Ax_a^2 \quad (18)$$

with the coefficient  $A > 0$  indicating the convexness. Reversely, we can rewrite  $x_a$  as a function of order parameter  $\tilde{T}_k$ :

$$x_a \simeq \tilde{T}_k - 2A\tilde{T}_k^2. \quad (19)$$

Moreover, for systems with  $E_b > 0$ , one can expect that there would be a fraction of collisions between active and inactive particles that do not induce activation. This effect leads to the elongation of the mean free path of activating collisions, or the decrease of the effective reactant density. Therefore, as a first-order approximation, we can have

$$\tilde{\rho}_r/\tilde{\rho} = 1 - B(1 - x_a)\tilde{E}_b \quad (20)$$

with the coefficient  $B > 0$ . Finally, by keeping only the first three leading terms, Eq. (15) can be written as

$$\frac{\partial \tilde{T}_k}{\partial \tilde{t}} = a\tilde{T}_k - b\tilde{T}_k^2 - c\tilde{T}_k^3 + h \quad (21)$$

with  $\tilde{t} = t/\tau_0$  and

$$a = \frac{\tilde{\rho}}{2}(1 - B\tilde{E}_b) - \frac{\tau_0}{\tau_d} \quad (22)$$

$$b = -\frac{\tilde{\rho}}{2} \left[ (1 + A)B\tilde{E}_b - A \right] \quad (23)$$

$$c = \frac{\tilde{\rho}}{2} \left[ 4A^2 + (3A - 4A^2)B\tilde{E}_b \right]. \quad (24)$$

$$h = \gamma\tau_0 dk_B T / (m\epsilon) \quad (25)$$

The solution of this cubic mean-field dynamic equation is given in the Appendix A. The corresponding phase diagram is summarized in Fig. 4. At zero thermal noise ( $T=0$ ) and  $E_b < E_{b,c}$  (or  $b > 0$ ), Eq. (21) has only one fixed point at  $a=0$  and the system undergoes a continuous phase transition with the mean-field critical exponent  $\beta_{\text{MF}}=1$  and upper critical dimension  $d_c=4$ . The transition points are shown as an orange curve in Fig. 4. In contrast, when  $E_b$  increases above  $E_{b,c}$  (or  $b < 0$ ), Eq. (21) has two fixed points, which corresponds to a bistability or a discontinuous dynamic phase transition. Importantly,  $E_b = E_{b,c}$  (or  $b=0$ ) is the tricritical point with  $\beta_{\text{MF}}=1/2$  and  $d_c=3$ , which separates the continuous and discontinuous phase transitions (purple point in Fig. 4). In the presence of thermal noise ( $T > 0$ ), the continuous phase transition is smeared out accompanied by the shrink of bistability region (enclosed by red and blue surfaces). This general picture is insensitive to the specific choice of coefficients  $A, B$  and agrees qualitatively with the simulation results.

### Reggeon-field simulations at zero thermal noise

Next we further go beyond the mean-field level and recover spatial-temporal fluctuations in our theory. At  $T=0$ , the density of the system is homogeneous. The only leading term in current  $\mathbf{J}$  of Eq. (11) is  $\nabla^2 \tilde{T}_k^l$ . Thus Eq. (11-12) can be rewritten as,

$$\frac{\partial \tilde{T}_k^l}{\partial \tilde{t}} = \mu \nabla^2 \tilde{T}_k^l + a\tilde{T}_k^l - b\tilde{T}_k^{l2} - c\tilde{T}_k^{l3} + \Lambda \sqrt{\tilde{T}_k} \eta(\mathbf{r}, t) \quad (26)$$

$$\frac{\partial}{\partial \tilde{t}} \tilde{\rho}_l = D \nabla^2 \tilde{T}_k^l, \quad (27)$$

where,  $a, b$  and  $c$  are functions of  $\tilde{\rho}_l(\mathbf{r}, t)$  based on Eq. (22-24). The second dynamic equation Eq. (27) now becomes the thermophoreis diffusion equation of the particles. Eq. (26-27), in fact, share the same formula as in the Reggeon-field theory of C-DP [53]. Since the criticality of dynamic equations does not depend on specific choice of parameters, the critical exponents for Eq. (26-27) should be the same as the standard Reggeon field theory in which  $b$  and  $\tilde{\rho}$  are the controlling parameters with  $a = a'\tilde{\rho}_l(\mathbf{r}, t) - a_0$ . Other parameters are simply set as  $a_0=1, a'=1, c=1, \lambda=1, \mu=D=1, \Lambda=1$  [53]. Since the noise term is multiplicative, we adopt a numerical method based on Fokker-Planck equation [54] to integrate the standard Reggeon fields equations on square or cubic lattices. This method has been used to obtain the accurate critical exponents for both directed percolation and C-DP [54], but not for the tricritical points. In Fig. 2c,d, the open symbols show the results from the field simulations, which behave essentially the same as the reactive hard-sphere system. In Fig. 5, we do the same finite size scaling analysis for 2D field systems to obtain the critical exponents at  $b=1$  and  $b=-0.92$  (tricritical point). Similar analysis for 3D field systems can be found in Fig. S4 in Ref. [47]. The obtained (tri)critical exponents are also given in Table I, which are consistent with those from the hard-sphere systems. Moreover, the upper critical dimension  $d_c=3$  at tricriticality is also confirmed both in 3D hard-sphere systems and field simulations (see Table I). This quantitative agreement further proves the validity of our theory and concludes that the critical behavior of the reactive hard-sphere model at the edge of continuous absorbing phase transition is the same as the tricritical C-DP.

### Criticality at finite thermal noise

Lastly, our theory predicts another critical line (the green line in Fig. 4) in the finite thermal temperature regime ( $T > 0$ ), which at mean-field level satisfies  $[a_c, b_c, \tilde{T}_{k,c}] = \left[ -3\left(\frac{h}{c}\right)^{2/3}, -3\left(\frac{h}{c}\right)^{1/3}, \left(\frac{h}{c}\right)^{1/3} \right]$ . Around the critical point  $[a_c, b_c]$ , we can find a direction in the  $(a, b)$  parameter space, i.e.,  $(\tilde{T}_{k,c}, 1)$ , along which Eq. (21) can be rewritten as

$$\frac{\partial \Delta \tilde{T}_k}{\partial \tilde{t}} \simeq -c \Delta \tilde{T}_k (\Delta \tilde{T}_k^2 + \tilde{T}_{k,c} \Delta b/c), \quad (28)$$

with  $\Delta \tilde{T}_k = \tilde{T}_k - \tilde{T}_{k,c}$  and  $\Delta b = b - b_c$  (see Appendix A). Therefore, for  $\Delta b < 0$ , the system has two stable fix points  $\Delta \tilde{T}_k \simeq \pm \sqrt{-\Delta b \tilde{T}_{k,c}/c}$ , which leads to  $\beta_{\text{MF}}=1/2$ . Eq. (28) also indicates that for  $T > 0$ , the system has an emergent  $\mathbb{Z}_2$  symmetry under the transformation ( $\Delta \tilde{T}_k \rightarrow -\Delta \tilde{T}_k$ ). Thus, this mean-field analysis suggests that phase transition for  $T > 0$  could be a Ising-type. A recent work by Korchinski et al. [55] has shown that in the

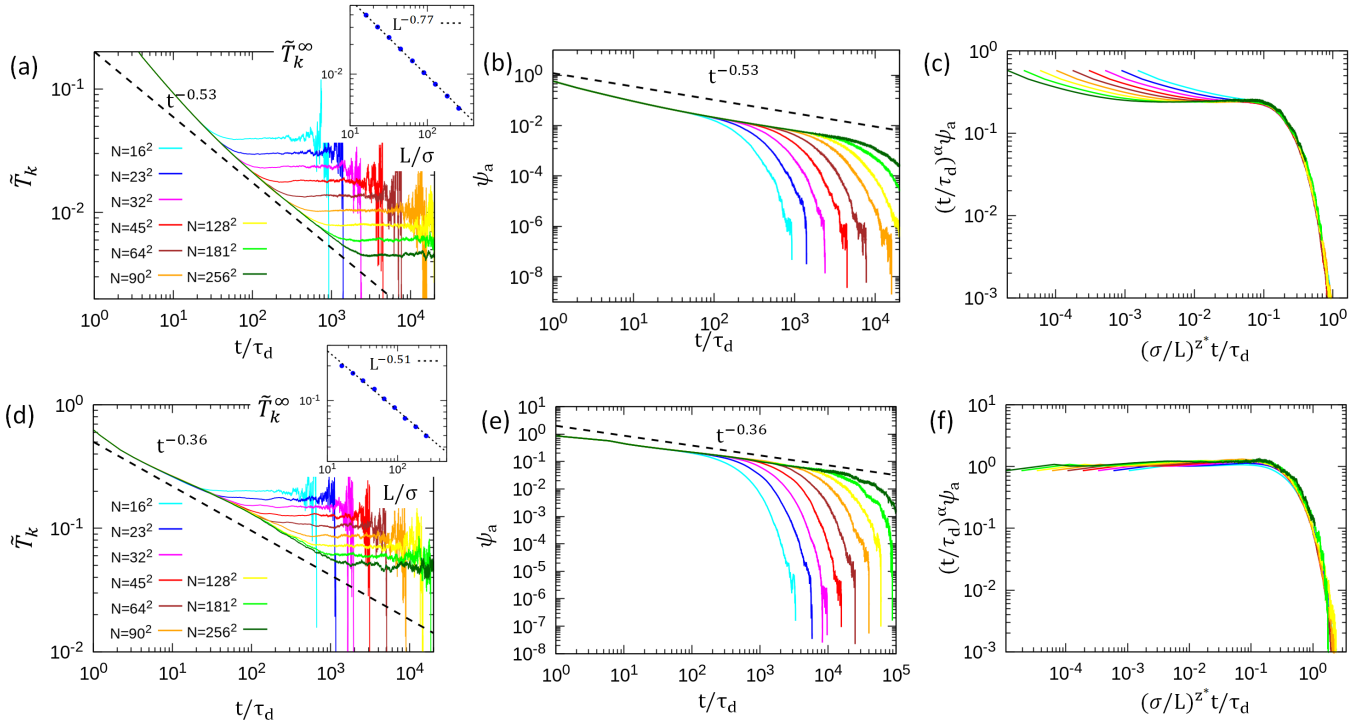


FIG. 5: Results for 2D field simulations. (a)  $\tilde{T}_k$  as a function of  $t$  for different system sizes with  $b=1$ ,  $\bar{\rho}=1.3722$ . (inset): saturated value as a function of system size  $L$ . (b) Overall activity  $\psi_a(t)$  for different system sizes. (c) Collapse of  $\psi_a(t)$  with  $\alpha=0.53$ ,  $z^*=1.51$ . (d)  $\tilde{T}_k$  as a function of  $t$  for different system sizes for 2D field simulation at tricritical point  $b=-0.92$ ,  $\bar{\rho}=0.8316$ . (e) Overall activity  $\psi_a(t)$  for different system sizes at  $b=-0.92$ . (f) Collapse of  $\psi_a(t)$  with  $\alpha=0.36$ ,  $z^*=1.65$ .

presence of thermal noise, the broken symmetry between space and time in DP can be partially restored, which gives rise to undirected-percolation-like critical behaviors. In fact, systems described by the dynamic equations for a non-conserved field coupled to a conserved field i.e., Eq (11-12), is categorised as dynamic model C according to Ref. [56]. Nevertheless, the relationship between the critical behaviors of non-equilibrium and the Ising universality has long been an active discussion topic in areas from chemical reactions [57–62], to dynamic network models [63–65], then to active fluids [14, 66, 67]. And we notice that our analysis for  $T > 0$  is different from recent theoretical works [64, 65], in which the authors concluded a DP-type of the transition by simply doing perturbation along the orthogonal directions in the  $(a, b)$  parameter space. Therefore, more numerical evidences are required to settle this issue.

## CONCLUSION AND DISCUSSION

In conclusion, by using simulation and theoretical analysis, we systematically investigate the criticality of a reactive hard sphere system with an activation barrier. We find that increasing the activation barrier effectively delays the dynamic transition but also increases the transition cooperativity which sharpens the transition. The

cooperativity enhancement comes from the interplay between activation barrier and the inertia of particles which make it possible for previous activation to facilitate the consecutive ones. This mechanism of barrier-controlled criticality has a direct implication for exothermic chemical reactions, where it was suggested that increasing the activation energy can make the reactions change from slow combustion to thermal explosion [68, 69]. Similar mechanism may also exist in nuclear chain reactions, which is highly relevant with the nuclear criticality safety [70]. Moreover, our finding is related with the dynamic phase transition in random organization systems. For examples, it was reported experimentally that for high density colloidal suspensions under oscillatory shearing, the geometrical protection from neighbouring particles suppresses or cancels the activated displacement, which sharpens the transition [28]. Similar discontinuous dynamic phase transitions have also been observed in driven amorphous solids [30, 34], the glass transition systems [71] and high-density active matter systems [41, 72]. In these cases, particles need to cross energy barriers or cages set by their neighbors to be activated. Therefore, our finding about the activation barrier on the criticality of a minimal reactive hard sphere model, can not only help understand the criticality of reactive particle systems, e.g., chemical reactions, but also shed lights in the dynamic behaviour of amorphous ma-

terials, active matter, as well as the spread of epidemic, knowledge and neural signals [5, 73, 74].

**Acknowledgments:** This work has been supported in part by the Singapore Ministry of Education through the Academic Research Fund MOE2019-T2-2-010 and RG104/17 (S), by Nanyang Technological University Start-Up Grant (NTU-SUG: M4081781.120), by the Advanced Manufacturing and Engineering Young Individual Research Grant (A1784C0018) and by the Science and Engineering Research Council of Agency for Science, Technology and Research Singapore, by the National Natural Science Foundation of China under Grant No. 11905001. We thank NSCC for granting computational resources.

## APPENDIX A: SOLUTION OF CUBIC DYNAMIC EQUATION

Considering the general cubic dynamic equation,

$$\frac{\partial \tilde{T}_k}{\partial \tilde{t}} = a\tilde{T}_k - b\tilde{T}_k^2 - c\tilde{T}_k^3 + h \quad (29)$$

In the case of zero conjugated field or thermal noise ( $h=0$ ), Eq.(29) have three steady states with  $\frac{\partial \tilde{T}_k}{\partial \tilde{t}} = 0$ ,

$$\tilde{T}_k = 0; \quad \tilde{T}_k = -\frac{b}{2c} \pm \sqrt{\frac{a}{c} + \left(\frac{b}{2c}\right)^2} \quad (30)$$

One can prove that when  $b > 0$ , the Eq.(29) shows a transcritical bifurcation and there is one fixed point, i.e.,

$$\tilde{T}_k = -\frac{b}{2c} + \sqrt{\frac{a}{c} + \left(\frac{b}{2c}\right)^2} \quad (31)$$

This corresponds to a second-order phase transition with critical scaling  $\tilde{T}_k \sim a^{\beta_{\text{MF}}}$  and critical exponent  $\beta_{\text{MF}} = 1$  as  $a \rightarrow 0$ . For  $b < 0$  the Eq.(29) has two fixed points, i.e.,

$$\tilde{T}_k = 0; \quad \tilde{T}_k = -\frac{b}{2c} + \sqrt{\frac{a}{c} + \left(\frac{b}{2c}\right)^2} \quad (32)$$

which corresponds to a bistability or a dis-continuous dynamic phase transition. Importantly,  $b=0$  is the tricritical point separating the continuous and dis-continuous phase transitions. At this point, the system exhibits supercritical pitchfork bifurcation and the mean-field tricritical scaling behavior changes into

$$\tilde{T}_k = \sqrt{\frac{a}{c}} \sim a^{\beta_{\text{MF}}^t} \quad (33)$$

with the mean-field tricritical exponent  $\beta_{\text{MF}}^t = 1/2$  different from the  $b > 0$  case. The upper critical dimension also

decreases from 4 in the previous one to 3 at this tricritical point [50]. For non-zero conjugated field ( $h > 0$ ), the boundary of the biastability region is determined by the following equation,

$$\left(\frac{h}{2c} - \frac{ab}{6c^2} - \frac{b^3}{27c^3}\right)^2 = \left(\frac{a}{3c} + \frac{b^2}{9c^2}\right)^3 \quad (b < 0, a < 0). \quad (34)$$

The theory also predicts a critical line as function of  $h > 0$ , i.e.,

$$b_c = -3 \left(\frac{h}{c}\right)^{1/3}; \quad a_c = -3 \left(\frac{h}{c}\right)^{2/3}; \quad \tilde{T}_{k,c} = \left(\frac{h}{c}\right)^{1/3}. \quad (35)$$

To obtain the mean-field critical exponent on this line, we do the perturbation of  $b$  around an arbitrary critical point on this line, i.e.,

$$b = b_c + \Delta b \quad (36)$$

$$\tilde{T}_k = \tilde{T}_{k,c} + \Delta \tilde{T}_k. \quad (37)$$

Based on Eq. (29), we have

$$\begin{aligned} \frac{\partial \tilde{T}_k}{\partial \tilde{t}} &= -c \left[ \tilde{T}_{k,c} + \Delta \tilde{T}_k - \left(\frac{h}{c}\right)^{1/3} \right]^3 - \Delta b (\tilde{T}_{k,c} + \Delta \tilde{T}_k)^2 \\ &\simeq -c \Delta \tilde{T}_k^3 - \Delta b \tilde{T}_{k,c}^2 = 0 \end{aligned} \quad (38)$$

which leads to the response of the order parameter

$$\Delta \tilde{T}_k \simeq - \left(\frac{\Delta b}{c}\right)^{1/3} \tilde{T}_{k,c}^{2/3} \quad (39)$$

A similar perturbation of  $a$  around the critical point gives

$$\Delta \tilde{T}_k \simeq \left(\frac{\Delta a}{c}\right)^{1/3} \tilde{T}_{k,c}^{1/3} \quad (40)$$

This leads to mean-field critical exponent  $\sigma_{\text{MF}}^{-1} = 1/3$ , the same as that in the mean-field Ising model. To obtain critical exponent  $\beta_{\text{MF}}$ , we do perturbation along the path  $\Delta a = \Delta b \tilde{T}_k^*$ . We have

$$\begin{aligned} \frac{\partial \Delta \tilde{T}_k}{\partial \tilde{t}} &= -c \Delta \tilde{T}_k^3 + \Delta a (\tilde{T}_{k,c} + \Delta \tilde{T}_k) - \Delta b (\tilde{T}_{k,c} + \Delta \tilde{T}_k)^2 \\ &= -c \Delta \tilde{T}_k^3 - \tilde{T}_{k,c} \Delta b \Delta \tilde{T}_k - \Delta b \Delta \tilde{T}_k^2 \\ &\simeq -c \Delta \tilde{T}_k (\Delta \tilde{T}_k^2 + \tilde{T}_{k,c} \Delta b / c) = 0 \end{aligned} \quad (41)$$

Therefore, if  $\Delta b < 0$ , the system has two stable fixed points with emergent  $\mathbb{Z}_2$  symmetry,

$$\Delta \tilde{T}_k \simeq \pm \sqrt{-\Delta b \tilde{T}_{k,c} / c}. \quad (42)$$

---

\* Electronic address: r.ni@ntu.edu.sg



- [1] Hinrichsen, H. Non-equilibrium critical phenomena and phase transitions into absorbing states. *Advances in physics* **49**, 815–958 (2000).
- [2] Henkel, M., Hinrichsen, H. & Lübeck, S. *Non-equilibrium phase transitions: Absorbing Phase Transitions*, vol. 1 (Springer, 2008).
- [3] Schlögl, F. Chemical reaction models for non-equilibrium phase transitions. *Zeitschrift für physik* **253**, 147–161 (1972).
- [4] Claycomb, J., Bassler, K., Miller Jr, J., Nersesyan, M. & Luss, D. Avalanche behavior in the dynamics of chemical reactions. *Phys. Rev. Lett.* **87**, 178303 (2001).
- [5] Pastor-Satorras, R., Castellano, C., Van Mieghem, P. & Vespignani, A. Epidemic processes in complex networks. *Rev. Mod. Phys.* **87**, 925 (2015).
- [6] Munoz, M. A. Colloquium: Criticality and dynamical scaling in living systems. *Rev. Mod. Phys.* **90**, 031001 (2018).
- [7] Pine, D. J., Gollub, J. P., Brady, J. F. & Leshansky, A. M. Chaos and threshold for irreversibility in sheared suspensions. *Nature* **438**, 997–1000 (2005).
- [8] Corte, L., Chaikin, P., Gollub, J. P. & Pine, D. Random organization in periodically driven systems. *Nat. Phys.* **4**, 420–424 (2008).
- [9] Regev, I., Weber, J., Reichhardt, C., Dahmen, K. A. & Lookman, T. Reversibility and criticality in amorphous solids. *Nat. Commun.* **6**, 8805 (2015).
- [10] Bak, P., Tang, C. & Wiesenfeld, K. Self-organized criticality: An explanation of the  $1/f$  noise. *Phys. Rev. Lett.* **59**, 381 (1987).
- [11] Takeuchi, K. A., Kuroda, M., Chaté, H. & Sano, M. Directed percolation criticality in turbulent liquid crystals. *Physical review letters* **99**, 234503 (2007).
- [12] Schaller, V., Weber, C. A., Hammerich, B., Frey, E. & Bausch, A. R. Frozen steady states in active systems. *Proc. Natl. Acad. Sci. U.S.A* **108**, 19183–19188 (2011).
- [13] Shi, X.-q. & Ma, Y.-q. Topological structure dynamics revealing collective evolution in active nematics. *Nat. Commun.* **4**, 3013 (2013).
- [14] Partridge, B. & Lee, C. F. Critical motility-induced phase separation belongs to the Ising universality class. *Phys. Rev. Lett.* **123**, 068002 (2019).
- [15] Sheinman, M., Sharma, A., Alvarado, J., Koenderink, G. & MacKintosh, F. Anomalous discontinuity at the percolation critical point of active gels. *Phys. Rev. Lett.* **114**, 098104 (2015).
- [16] Hu, H., Ziff, R. M. & Deng, Y. No-enclave percolation corresponds to holes in the cluster backbone. *Phys. Rev. Lett.* **117**, 185701 (2016).
- [17] Harris, T. E. Contact interactions on a lattice. *The Annals of Probability* 969–988 (1974).
- [18] Manna, S. Two-state model of self-organized criticality. *J. Phys. A: Math. Gen.* **24**, L363 (1991).
- [19] Rossi, M., Pastor-Satorras, R. & Vespignani, A. Universality class of absorbing phase transitions with a conserved field. *Phys. Rev. Lett.* **85**, 1803 (2000).
- [20] Chou, D.-P. & Yip, S. Computer molecular dynamics simulation of thermal ignition in a self-heating slab. *Combustion and Flame* **47**, 215–218 (1982).
- [21] Chou, D.-P. & Yip, S. Molecular dynamics simulation of thermal ignition in a reacting hard sphere fluid. *Combustion and flame* **58**, 239–253 (1984).
- [22] Baras, F. & Mansour, M. M. Validity of macroscopic rate equations in exothermic chemical systems. *Phys. Rev. Lett.* **63**, 2429 (1989).
- [23] Nowakowski, B. & Lemarchand, A. Stochastic effects in a thermochemical system with newtonian heat exchange. *Phys. Rev. E* **64**, 061108 (2001).
- [24] Semenov, N. Theories of combustion process. *Z. Phys. Chem.* **48**, 571–582 (1928).
- [25] Semenov, N. *Some Problems of Chemical Kinetics and Reactivity*, vol. 1 & 2 (1959).
- [26] Corte, L., Gerbode, S., Man, W. & Pine, D. Self-Organized Criticality in Sheared Suspensions. *Phys. Rev. Lett.* **103**, 248301 (2009).
- [27] Franceschini, A., Filippidi, E., Guazzelli, E. & Pine, D. J. Transverse alignment of fibers in a periodically sheared suspension: an absorbing phase transition with a slowly varying control parameter. *Phys. Rev. Lett.* **107**, 250603 (2011).
- [28] Jeanneret, R. & Bartolo, D. Geometrically protected reversibility in hydrodynamic Loschmidt-echo experiments. *Nat. Commun.* **5**, 1–8 (2014).
- [29] Leishangthem, P., Parmar, A. D. & Sastry, S. The yielding transition in amorphous solids under oscillatory shear deformation. *Nature communications* **8**, 1–8 (2017).
- [30] Das, P., Vinutha, H. & Sastry, S. Unified phase diagram of reversible–irreversible, jamming, and yielding transitions in cyclically sheared soft-sphere packings. *Proceedings of the National Academy of Sciences* **117**, 10203–10209 (2020).
- [31] Ness, C. & Cates, M. E. Absorbing-state transitions in granular materials close to jamming. *Physical Review Letters* **124**, 088004 (2020).
- [32] Milz, L. & Schmiedeberg, M. Connecting the random organization transition and jamming within a unifying model system. *Phys. Rev. E* **88**, 062308 (2013).
- [33] Zhou, C., Reichhardt, C. O., Reichhardt, C. & Beyerlein, I. Random organization in periodically driven gliding dislocations. *Physics Letters A* **378**, 1675–1678 (2014).
- [34] Nagasawa, K., Miyazaki, K. & Kawasaki, T. Classification of the reversible–irreversible transitions in particle trajectories across the jamming transition point. *Soft matter* **15**, 7557–7566 (2019).
- [35] Mangan, N., Reichhardt, C. & Reichhardt, C. O. Reversible to irreversible flow transition in periodically driven vortices. *Phys. Rev. Lett.* **100**, 187002 (2008).
- [36] Reichhardt, C. & Reichhardt, C. O. Random organization and plastic depinning. *Phys. Rev. Lett.* **103**, 168301 (2009).
- [37] Okuma, S., Tsugawa, Y. & Motohashi, A. Transition from reversible to irreversible flow: Absorbing and depinning transitions in a sheared-vortex system. *Phys. Rev. B* **83**, 012503 (2011).
- [38] Hexner, D. & Levine, D. Hyperuniformity of critical absorbing states. *Phys. Rev. Lett.* **114**, 110602 (2015).
- [39] Tjhung, E. & Berthier, L. Hyperuniform density fluctuations and diverging dynamic correlations in periodically driven colloidal suspensions. *Phys. Rev. Lett.* **114**, 148301 (2015).
- [40] Weijs, J. H., Jeanneret, R., Dreyfus, R. & Bartolo, D. Emergent hyperuniformity in periodically driven emulsions. *Phys Rev Lett* **115**, 108301 (2015).
- [41] Lei, Q.-L., Ciamarra, M. P. & Ni, R. Nonequilibrium strongly hyperuniform fluids of circle active particles with large local density fluctuations. *Sci. Adv.* **5**, eaau7423 (2019).
- [42] Lei, Q.-L. & Ni, R. Hydrodynamics of random-organizing

- hyperuniform fluids. *Proc. Natl. Acad. Sci. U.S.A* **116**, 22983–22989 (2019).
- [43] Ma, Z. & Torquato, S. Hyperuniformity of generalized random organization models. *Physical Review E* **99**, 022115 (2019).
- [44] Rapaport, D. C. *The art of molecular dynamics simulation* (Cambridge university press, 2004).
- [45] Scala, A. Event-driven Langevin simulations of hard spheres. *Phys. Rev. E* **86**, 026709 (2012).
- [46] Achlioptas, D., D’Souza, R. M. & Spencer, J. Explosive percolation in random networks. *Science* **323**, 1453–1455 (2009).
- [47] See Supplemental Material at [URL] for the simulation results of 3D reactive particle systems and results of 3D field simulation.
- [48] Basu, M., Basu, U., Bondyopadhyay, S., Mohanty, P. & Hinrichsen, H. Fixed-energy sandpiles belong generically to directed percolation. *Phys. Rev. Lett.* **109**, 015702 (2012).
- [49] Lee, S. B. Comment on “fixed-energy sandpiles belong generically to directed percolation”. *Phys. Rev. Lett.* **110**, 159601 (2013).
- [50] Lübeck, S. Tricritical directed percolation. *J Stat Phys* **123**, 193–221 (2006).
- [51] Janssen, H.-K., Müller, M. & Stenull, O. Generalized epidemic process and tricritical dynamic percolation. *Phys. Rev. E* **70**, 026114 (2004).
- [52] Araújo, N. A., Andrade Jr, J. S., Ziff, R. M. & Herrmann, H. J. Tricritical point in explosive percolation. *Phys. Rev. Lett.* **106**, 095703 (2011).
- [53] di Santo, S., Burioni, R., Vezzani, A. & Muñoz, M. A. Self-organized bistability associated with first-order phase transitions. *Phys. Rev. Lett.* **116**, 240601 (2016).
- [54] Dornic, I., Chaté, H. & Muñoz, M. A. Integration of Langevin equations with multiplicative noise and the viability of field theories for absorbing phase transitions. *Phys. Rev. Lett.* **94**, 100601 (2005).
- [55] Korchinski, D. J., Orlandi, J. G., Son, S.-W. & Davidsen, J. Criticality in spreading processes without time-scale separation and the critical brain hypothesis. *arXiv e-prints* arXiv:1908 (2019).
- [56] Hohenberg, P. C. & Halperin, B. I. Theory of dynamic critical phenomena. *Rev. Mod. Phys.* **49**, 435 (1977).
- [57] Dewel, G., Walgraef, D. & Borckmans, P. Renormalization group approach to chemical instabilities. *Zeitschrift für Physik B Condensed Matter* **28**, 235–237 (1977).
- [58] Brachet, M. & Tirapegui, E. On the critical behaviour of the Schlögl model. *Phys. Lett. A* **81**, 211–214 (1981).
- [59] Dewel, G., Borckmans, P. & Walgraef, D. Nonequilibrium phase transitions and chemical instabilities. *J. Stat. Phys.* **24**, 119–137 (1981).
- [60] Grassberger, P. On phase transitions in Schlögl’s second model. In *Nonlinear Phenomena in Chemical Dynamics*, 262–262 (Springer, 1981).
- [61] Tomé, T. & Dickman, R. Ziff-Gulari-Barshad model with CO desorption: An Ising-like nonequilibrium critical point. *Phys. Rev. E* **47**, 948 (1993).
- [62] Liu, D.-J., Pavlenko, N. & Evans, J. W. Crossover between mean-field and Ising critical behavior in a lattice-gas reaction-diffusion model. *J. Stat. Phys.* **114**, 101–114 (2004).
- [63] Majdandzic, A. *et al.* Spontaneous recovery in dynamical networks. *Nat. Phys.* **10**, 34–38 (2014).
- [64] Böttcher, L., Nagler, J. & Herrmann, H. J. Critical behaviors in contagion dynamics. *Phys. Rev. Lett.* **118**, 088301 (2017).
- [65] Böttcher, L., Luković, M., Nagler, J., Havlin, S. & Herrmann, H. J. Failure and recovery in dynamical networks. *Sci. Rep.* **7**, 1–9 (2017).
- [66] Siebert, J. T. *et al.* Critical behavior of active Brownian particles. *Physical Review E* **98**, 030601 (2018).
- [67] Dittrich, F., Speck, T. & Virnau, P. Critical behaviour in active lattice models of motility-induced phase separation. *arXiv preprint arXiv:2010.08387* (2020).
- [68] Boddington, T., Gray, P. & Robinson, C. Thermal explosions and the disappearance of criticality at small activation energies: exact results for the slab. *Proceedings of the Royal Society of London. A. Mathematical and Physical Sciences* **368**, 441–461 (1979).
- [69] Lacey, A. Critical behaviour of homogeneous reacting systems with large activation energy. *Int. J. Eng. Sci.* **21**, 501–515 (1983).
- [70] Lamarsh, J. R. & Baratta, A. J. *Introduction to nuclear engineering*, vol. 3 (Prentice hall Upper Saddle River, NJ, 2001).
- [71] Hedges, L. O., Jack, R. L., Garrahan, J. P. & Chandler, D. Dynamic order-disorder in atomistic models of structural glass formers. *Science* **323**, 1309–1313 (2009).
- [72] Tjhung, E. & Berthier, L. Discontinuous fluidization transition in time-correlated assemblies of actively deforming particles. *Phys. Rev. E* **96**, 050601 (2017).
- [73] Dodds, P. S. & Watts, D. J. Universal behavior in a generalized model of contagion. *Phys. Rev. Lett.* **92**, 218701 (2004).
- [74] Gerstner, W. & Kistler, W. M. *Spiking neuron models: Single neurons, populations, plasticity* (Cambridge university press, 2002).